5th IAA Planetary Defense Conference – PDC 2017
15-19 May 2017, Tokyo, Japan

IAA-PDC-17-04-03

CHARACTERISTICS OF A HIGH-POWER ION BEAM DEFLECTION SYSTEM NECESSARY TO DEFLECT THE HYPOTHETICAL ASTEROID 2017 PD

John Brophy(1), **Nathan Strange**(2), **Dan Goebel**(3) **Shawn Johnson**(4), **Dan Mazanek**(5) **and David Reeves**(6)
(1)(2)(3)(4)*Jet Propulsion Laboratory, California Institute of Technology, Pasadena, CA*
818-254-0446, John.R.Brophy@jpl.nasa.gov
(5)(6)*NASA Langley Research Center, Hampton, VA*
757-864-1739, Daniel.D.Mazanek@nasa.gov

Keywords: *Ion beam deflection, ion shepherd, solar electric propulsion*

ABSTRACT

The July 2027 impact date for the hypothetical asteroid 2017 PDC, that is the subject of an emergency response exercise, leaves just over ten years to implement a deflection approach. The analyses herein allocates four years to the design, fabrication, assembly, test and launch of a notional high-power Ion Beam Deflection (IBD) vehicle to meet a launch readiness date no later than May 2021. Using this launch date along with estimates for the vehicle mass and performance characteristics of the electric propulsion system, low-thrust trajectory analyses indicate a 2.56-year flight time to rendezvous with 2017 PDC. This would leave 3.6 years to execute the actual deflection phase. A 160-kW IBD vehicle could deflect 2017 PDC by at least one Earth radius within this time provided the asteroid's actual diameter was less than about 140 m and its density was 2 g/cm^3 or less. Larger diameters and/or higher densities would require a higher power IBD vehicle, multiple IBD vehicles, or a longer deflection phase. Ion beam deflection is largely independent of the characteristics of the threat object, but its effectiveness, like all deflection approaches, is sensitive to both the asteroid mass and the time available for deflection. The characteristics of IBD, i.e., large standoff distance between the spacecraft and the asteroid surface, as well as ion beam divergence angles of a few degrees, facilitates the possible simultaneous use of multiple IBD vehicles to improve the performance and robustness of the asteroid deflection. The 65-cm diameter, 20-kW NEXIS ion thruster developed in support of the Jupiter Icy Moons Orbiter mission concept is particularly well suited for application to a high-power IBD system. It has demonstrated an ion beam divergence angle of approximately 2 degrees and operation at 20 kW for over 2,000 hours. Completion of the development and flight qualification of this technology would significantly reduce the risk and time necessary to respond to the discovery of potentially hazardous asteroid in the size range of 50- to 100-m diameter.

Introduction

Solar electric propulsion (SEP) is now used extensively in the commercial communication satellite industry and it has been used successfully on a handful of deep-space science missions including: Deep Space 1, SMART-1, Dawn, Hayabusa 1, and Hayabusa 2 [1-5]. The unique performance capabilities of SEP make it attractive for missions that require a large post-launch spacecraft velocity change, ΔV. For example, the ion propulsion system on the Dawn spacecraft provided a ΔV of 11 km/s, roughly four times the highest ΔV provided by any onboard chemical propulsion system used in deep space. NASA is now considering the use of high-power SEP as an integral part of its plans to extend human exploration beyond low Earth orbit [6], with power levels in the range of 40 kW to > 150 kW. This paper presents the potential

capabilities of a conceptual ion beam deflection (IBD) system using high-power SEP to deflect the hypothetical asteroid 2017 PD. Power levels in the range of tens to hundreds of kilowatts are considered.

Ion beam deflection works by directing a beam of high-energy ions into the surface of the threat object, as indicated in Fig. 1, and transferring the momentum of the ions to the object through inelastic collisions [7-9]. This is conceptually similar to a kinetic impactor with the impinging ions taking the place of the impacting spacecraft, but with two important differences. First, an ion beam deflection system can be designed so that the ions impact the asteroid surface at speeds much greater than is practical for kinetic impactor and in the direction most effective for deflection. Ion impact speeds of 70 km/s are readily achievable, which would be roughly four to five times the impact speed of a kinetic impactor spacecraft. Second, finite power levels for the IBD vehicle means the transfer of momentum is necessarily spread out over time, typically over a timescale of months to years. The first difference above suggests that IBD could be more effective than a typical kinetic impactor while the second difference suggests the opposite.

The potential impact of asteroid 2017 PDC in July 2027 leaves just over ten years to develop and launch the spacecraft, rendezvous with the asteroid, and perform the deflection maneuver. We determine the system power level and the characteristics of the electric thrusters necessary to transport the conceptual IBD vehicle to the asteroid and perform the deflection activity within the available time. The same electric propulsion system is assumed be used for both transportation of the IBD vehicle to the asteroid and for the deflection activity.

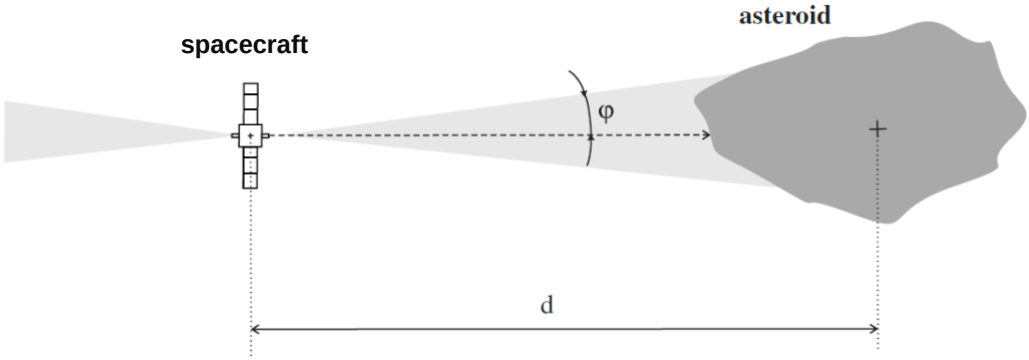

Fig. 1 Basic ion beam deflection configuration (from Ref. 7).

IBD Characteristics

We divide the time available to deflect 2017 PDC into three phases:

1. Vehicle Development Phase: In this phase the IBD spacecraft would be designed, assembled, tested, and fueled. It would end with the spacecraft launched to Earth escape.
2. Rendezvous Phase: This phase would begin immediately after the launch of the IBD vehicle to Earth escape and end with the spacecraft at the asteroid ready to begin the deflection phase. Most of the time in this phase would be spent using the ion propulsion system to perform the heliocentric transfer of the spacecraft to the asteroid.
3. Deflection Phase: In this phase, the ion beam deflection system would be used to push the asteroid over a time period of months to years.

The driving requirements for the notional IBD vehicle are include:

1. Minimize the flight time to rendezvous with the asteroid.
2. Deliver sufficient propellant to accomplish the asteroid deflection.

3. Process all of the available power from the solar array in a reasonable number of thrusters.
4. Maximize the separation distance between the asteroid surface and the IBD vehicle.
5. Maximize the fraction of the momentum in the ion beam delivered to the asteroid.
6. Have a sufficient power throttling range to enable operation over the required variation in solar range during all phases of the mission.
7. Have sufficient thruster lifetime to perform the asteroid deflection phase without the use of additional thrusters.

Development Phase

Four years is allocated to the vehicle development phase. This is a realistic, if somewhat aggressive schedule that assumes six-month durations each for development phases A and B, and three years for phase C/D. This leaves a little more than six years for the rendezvous and deflection phases.

Maximizing the separation distance from the asteroid surface is necessary to minimize the gravitational attraction between the asteroid and the spacecraft and to minimize the rate of material sputtered from the asteroid surface by the ion beam that is deposited on the spacecraft. Meeting this requirement while maximizing the fraction of momentum in the ion beam delivered to the asteroid requires an electric thruster that can produce an ion beam with a very small beam divergence angle. The diameter of the ion beam as a function of the distance to the asteroid surface is given in Fig. 2 for ion beam divergence angles of 2 to 4 degrees. For asteroid diameters in the range 100 m to 250 m, it is clear that the thruster must produce a beam divergence angle of ~4 degrees or less in order to enable spacecraft-to-asteroid-surface separation distances of greater than ~500 m.

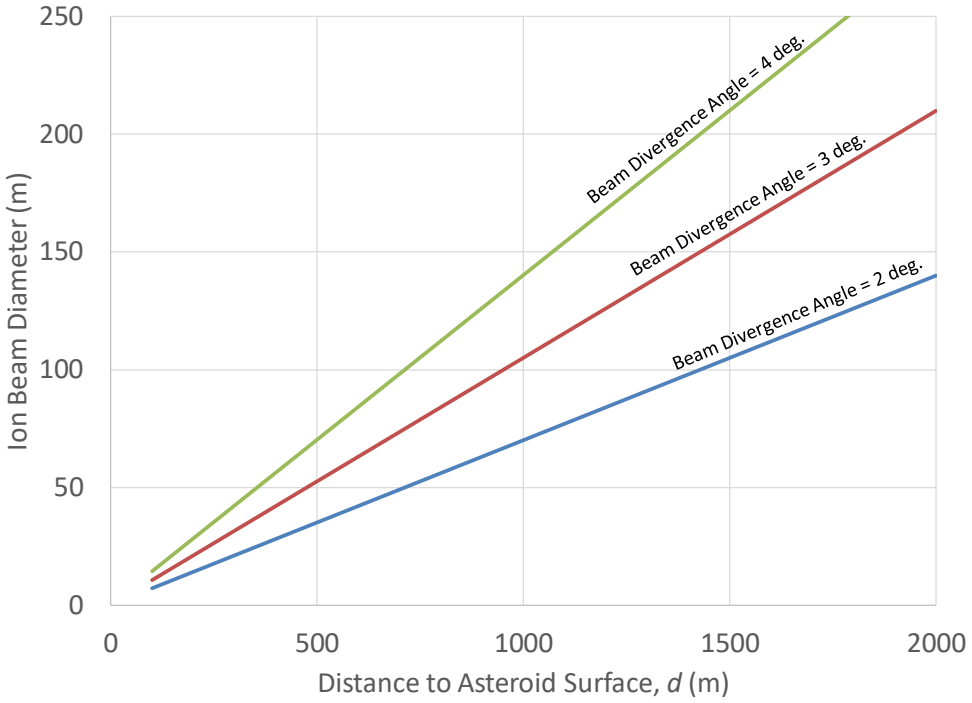

Fig. 2 Ion beam divergence angles of ≤ 4 degrees are necessary to enable spacecraft-to-asteroid-surface separation distances greater than 500 m and have the ion beam diameter be less than asteroid diameter in the range 100 m to 250 m (assuming spherical asteroids).

There are numerous types of electric thrusters either currently flying or under development including resistojet, arcjets, pulsed plasma thrusters, Hall thrusters, magnetoplasmadynamic thrusters, and gridded ion thrusters, but only gridded ion thrusters are capable of producing the required ion beam divergence angles. Equipped with appropriately designed ion optics, gridded ion thrusters can produce ion beams with divergence angles of just a few degrees. This type of thruster is also capable of high-power operation, a large input power throttling range, and long life.

The NEXIS ion thruster [10] was developed in support of the Jupiter Icy Moons Orbiter (JIMO) mission concept and has all of the characteristics needed for a high-power IBD vehicle. When equipped with flat, carbon-carbon grids, it has demonstrated a small ion beam divergence angle as indicated qualitatively in Fig. 3. A development model NEXIS ion thruster was subjected to a 2,000-hr wear test at the performance characteristics given in Table 1 [10]. This development model thruster also successfully passed vibration testing at protoflight levels. The NEXIS thruster is considered mature enough to proceed to engineering model development with only minor modifications. It had a design life requirement of 10 years, which far exceeds the time available for the deflection of asteroid 2017 PDC.

Table 1 NEXIS Thruster Characteristics

Parameter	Value
Input Power	20.4 kW
Thrust	446 mN
Specific Impulse	7050 s
Thruster Efficiency	0.757
Ion Beam Voltage	4750 V
Ion Beam Current	4.08 A

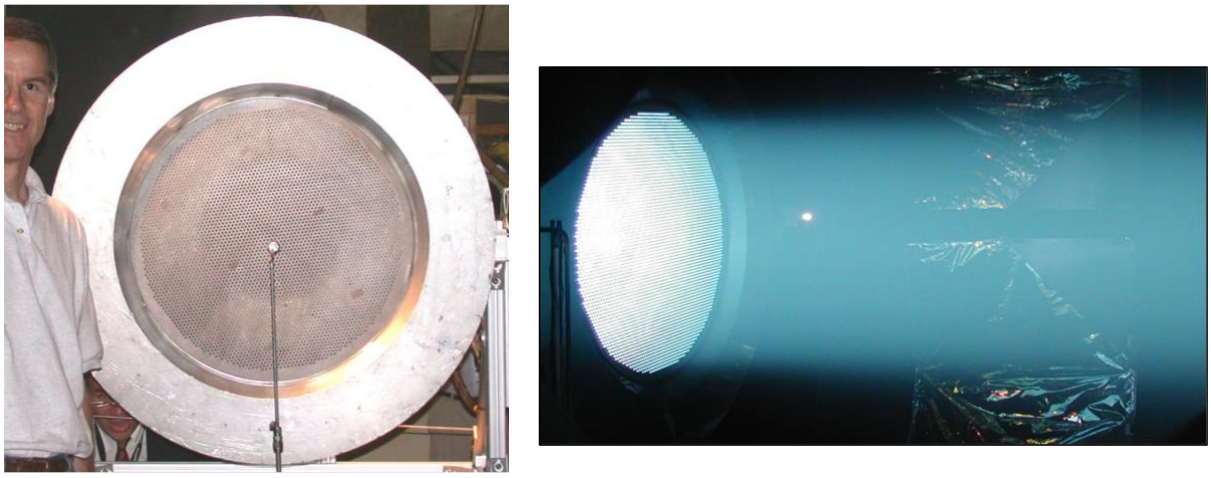

Fig. 3 The 65-cm diameter, 20-kW, NEXIS ion thruster (left) equipped with flat carbon-carbon grids demonstrates operation with a small ion beam divergence angle (right).

Rendezvous Phase

Like all slow-push planetary defense techniques, IBD requires the vehicle to rendezvous with the threat object. In order to maximize the time available for the deflection phase, it is necessary to minimize the rendezvous trip time. To accomplish this the IBD vehicle would be designed so that the electric propulsion system could use all of the available power during the transfer phase (Fig. 4 left). During the subsequent deflection phase, the vehicle would be reconfigured into the IBD configuration so that it could thrust both toward and away from the asteroid simultaneously (Fig. 4 right). The IBD configuration would be maintained until the desired deflection is verified. Thrusting in the direction away from the asteroid is necessary to maintain station-keeping of the spacecraft relative to the asteroid. During the IBD phase, the

flight system would continuously enforce equal and opposite forces and zero torques by reorienting the spacecraft and steering the net thrust vector through the time-varying center of mass.

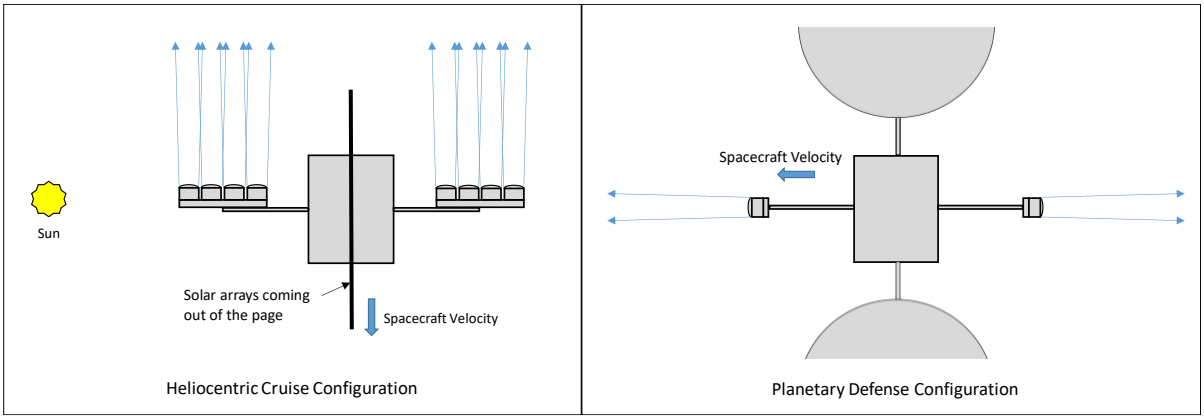

Fig. 4 The IBD vehicle would be configured to use all of the available power for the heliocentric transfer to the asteroid (left) and then be reconfigured to enable thrusting in opposite directions during the IBD phase (right).

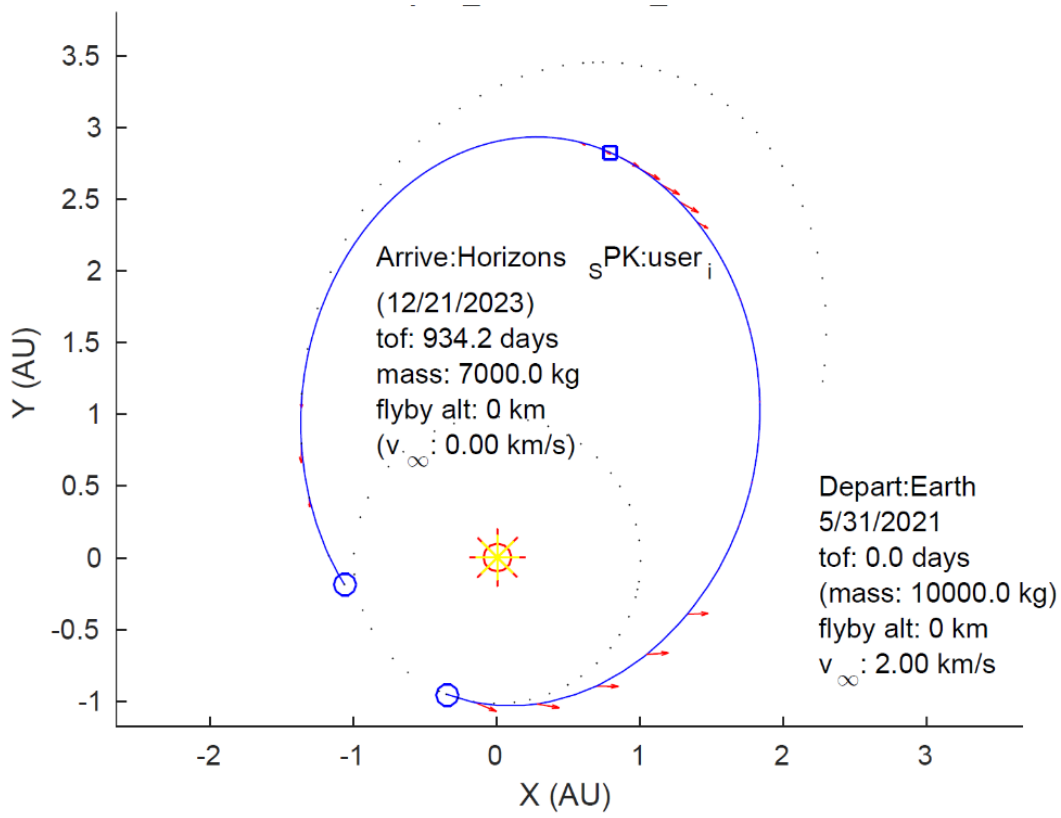

Fig. 5 Rendezvous trajectory to 2017 PDC for a Falcon Heavy launch of a 10,000-kg IBD spacecraft. The notional spacecraft is assumed to have solar electric propulsion system that can process up to 160 kW at specific impulse of 7,000 s. The overall IBD vehicle dry mass is given in Table 2.

To determine the duration of the rendezvous phase we selected a maximum input power level to the electric propulsion system of 160 kW and estimated the corresponding spacecraft dry mass given in Table 2. These values were then used in a low-thrust trajectory analysis to determine how long it would take to rendezvous with 2017 PDC assuming a launch readiness date no earlier than May 2021. The results, given in Fig. 5, indicate a 2.56-year flight time with a delivered mass of 7,000 kg from an initial mass of 10,000 kg launched with a Falcon-Heavy-like launcher to a V_∞ of 2 km/s. The trajectory in Fig. 5 indicates that it would take 3,000 kg of xenon to deliver the IBD vehicle the asteroid. The mass estimate in Table 2 indicates that the vehicle can carry a total of xenon mass of 4700 kg. Allocating 6% of this for contingency and subtracting 3,000 kg used for the rendezvous phase leaves 1,400 kg for the deflection phase. With contingency and margin the beginning-of-life solar array power level at 1 AU is assumed to be 184 kW in order to provide 160 kW to the IBD system at end-of-life at 1 AU. The mass estimates in Table 2 are scaled from the mass estimates in NASA's Asteroid Redirect Robotic Mission reference spacecraft design.

IBD Performance for 2017 PDC

The trajectory in Fig. 5 has the IBD spacecraft arriving at the asteroid on December 21, 2023 leaving 3.6 years for the IBD deflection phase. To calculate the amount of deflection the IBD vehicle could provide, we integrate $\frac{\partial \zeta}{\partial A}$ over the duration of the low thrust deflection phase, where ζ is the position in the 2027 b-plane and A is the along-track direction. Paul Chodas [11] provided partial derivatives of the b-plane locations ξ and ζ with respect to velocity in ACN-space, where A is along-track (parallel to velocity vector), C is cross-track and N is normal, for asteroid 2017 PDC. Integration of $\frac{\partial \zeta}{\partial A}$ was performed numerically by calculating the deflection for each day assuming a constant applied thrust over that day and then summing over the number of thrusting days. The applied thrust was calculated based on the available power, which was conservatively assumed to vary with solar range as $1/r^2$. Upper and lower limits on the power that the electric propulsion system could process were established in order to facilitate the design and development of the propulsion system. If the available power exceeded the upper limit, then the propulsion system was assumed to operate at the upper limit. Thrusting was not allowed if the available power was less than the lower limit.

The deflection capability of the 160-kW IBD system is given in Fig. 6, where the ζ-deflection in the 2027 b-plane is plotted as a function of time before impact. These curves assume that the IBD system is thrusting 100% of the time during the deflection phase up to 45 days before the original impact date. The analysis assumes no thrusting during the last 45 days because it would not be beneficial to do so. Four asteroid cases are shown in Fig. 6 corresponding to asteroid diameters of 100 m, 150 m, 200 m and 250 m, where in each case an asteroid density of 2 g/cm^3 is assumed.

The vertical line in Fig. 6 indicates the point in time 3.6 years before impact. This corresponds to the arrival date of the IBD vehicle at the asteroid for the trajectory given in Fig. 5. Note the steep decline in the b-plane deflection distance if the deflection phase begins to the left of this line. This suggests that deflection operations must be started immediately upon arrival at the asteroid. Alternatively, if the spacecraft arrival date at the asteroid could be moved earlier by up to two years, so that it would arrive up to 6 years before impact, it would provide little additional deflection benefit. This is because between 6 and 4.5 years before impact the asteroid is greater than 3 AU from the sun and there is insufficient power to operate the IBD system as indicated in Fig. 7.

Table 2 160-kW IBD Vehicle Mass Estimate

	Unit Mass Max. Expected Value (kg)	Number of Units	Maximum Expected Value (CBE plus MGA) (kg)
Sensors			**40**
NFOV Camera	20	1	20
PD Sensor	10	2	20
C&DH	**21**	**1**	**21**
GNC			**18**
MIMU (2)	5	2	10
Star Trackers (2)	3	2	6
Sun Sensors (8)	0.25	8	2
Telecom			**38**
Small Deep Space Transponder (2)	3.5	2	7
100 W X-band TWTA (2)	2.5	2	5
1.8-m High Gain Antenna (1)	10	1	10
X-band Low Gain Antenna (3)	1	3	3
X-band Components	13	1	13
Power			**1417**
Solar Array (184-kW BOL at 1 AU, assuming 150 W/kg)	613	2	1227
Solar Array Boom	10	2	20
HV Down Converter (2)	20	2	40
HV Power Distribution Unit (1)	40	1	40
LV Power Distribution Unit (1)	20	1	20
Li-ion batteries (145 A-hrs)	70	1	70
Structure			**599**
Primary Structure (5% of Wet Mass)	500	1	500
Secondary Structure (10% of Primary Structure)	50	1	50
Brackets & Misc. Hardware (10% of Primary Structure)	50	1	50
Mechanisms			**342**
Solar Array Drive Assembly & Twist Capsule (2)	73.6	2	147
Hall Thruster Gimbal Assembly (40% of thruster mass)	12	10	120
Hall Thruster IBD Deployment Mechanism	25	2	50
HGA Gimbal Assembly	25	1	25
Thermal			**575**
Radiators (25 kg/kW)	230	1	230
MLI (~1.0x radiator mass)	230	1	230
Heaters, temp sensors, coatings, etc. (~1/2 radiator mass)	115	1	115
Electric Propulsion			**1005**
Ion Thruster (NEXIS)	30	10	300
Power Processor Unit (NEXIS)	40	10	400
Xenon Flow Controller	4	10	40
Xenon Tank (5% of xenon mass)	235	1	235
Xenon Regulator	1.5	2	3
Latch Valve	0.5	2	1
Service Valve	0.2	3	1
Propellant Lines & Fittings	25	1	25
Chemical Propulsion			**62**
22N Hydrazine Thruster	0.6	16	10
Hydrazine Tank	33	1	33
Brackets & propellant lines	15	1	15
Filter	0.9	1	1
Pressdure Transducer	0.25	3	1
Latch Valve	0.6	2	1
Service Valve	0.23	4	1
Pyro Valve	0.21	2	0
Harness (7% of dry mass MEV)	**310**	**1**	**316**
Flight System Dry (MEV)			**4427**
System Margin (15%)			**656**
Total Flight System Dry Mass			**5091**
Xenon			4700
Hydrazine			200
Total Flight System Wet Mass			**9991**

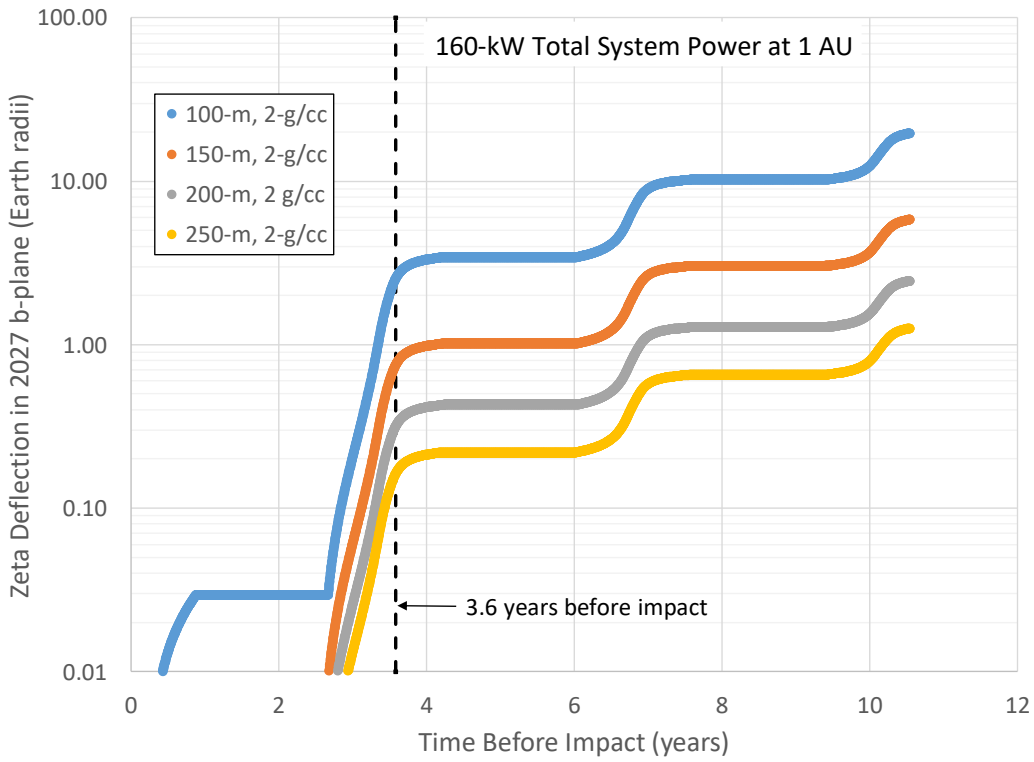

Fig. 6 Illustration of the deflection capability of a 160-kW IBD system.

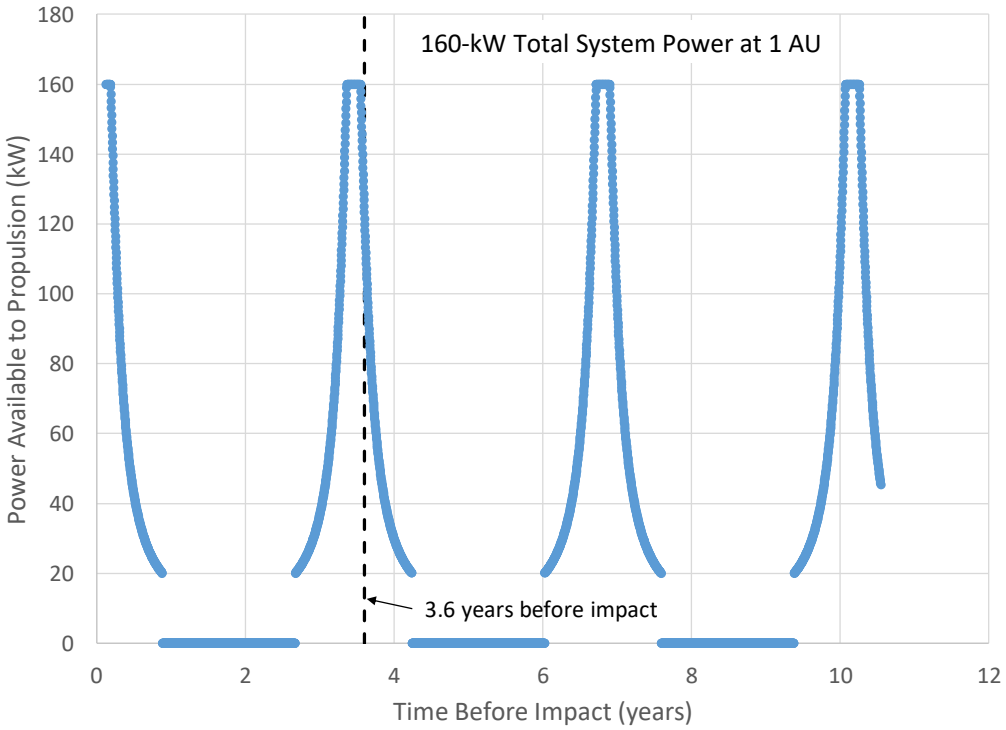

Fig. 7 Power available to the IBD propulsion system for the 160-kW spacecraft used in deflection results given in Fig. 4. The upper power limit is clipped at 160 kW and the lower limit is set to 20 kW corresponding to the operation of two NEXIS thrusters throttled down to 10 kW each.

The blue curve in Fig. 6 indicates that as long as the 160-kW IBD vehicle begins the deflection phase no later than 3.6 years before impact, it could deflect asteroid 2017 PDC by over two Earth radii, assuming the asteroid is 100-m diameter and has a density ≤ 2 g/cm^3. Similarly, the orange curve indicates that the 160-kW IBD vehicle could deflect 2017 PDC by up to one Earth radii, if it was up to 150-m diameter and ≤ 2 g/cm^3 provided deflection operations could begin no later than four years before impact. To deflect sizes up to 200-m diameter, with densities ≤ 2 g/cm^3, by one Earth radii would require initiation of the IBD deflection phase no later than about seven years before impact. Although these longer deflection times are not consistent with the 4-year development phase and 2.56-year rendezvous phase durations.

The total ΔV that the IBD system could put into the asteroid is given in Fig. 8. These curves indicate that the IBD system could provide a ΔV of roughly 4 cm/s to the 100-m asteroid size for deflection operations beginning 3.6 years before impact. Similarly, the system could provide approximately 1 cm/s ΔV to a 150-m asteroid. If the asteroid density is less than 2 g/cm^3, the total ΔV's will be greater. The propellant required for the 160-kW IBD system is given as a function of deflection time in Fig. 9. For IBD operations beginning 3.6 years before impact 1200 kg of xenon would required, which is less than the 1400 kg available.

In addition to the 160-kW IBD vehicle, we also evaluated the potential performance of 60-kW and 320-kW IBD spacecraft. The deflection capability of the 60-kW IBD system and the corresponding power variation with time are given in Figs. 10 and 11. Similarly, the deflection and power curves for a 320-kW IBD vehicle are given in Figs. 12 and 13. It is clear from Fig. 10 that the 60-kW IBD vehicle could deflect asteroids up to 100-m diameter with densities up to 2 g/cm^3 within the 3.6 years of time available for deflection. The power curve in Fig. 11 indicates relatively short periods of time where there is sufficient power available to the IBD system. This is primarily the result of the assumption that the minimum power per NEXIS thruster is 10 kW and two must be operated simultaneously during IBD operations. The corresponding performance of a 320-kW IBD system given in Fig. 12. Such a system could deflect a 150-m asteroid at up to 2 g/cm^3 by nearly two Earth radii within the 3.6 years available, but falls short of deflecting a 200-m diameter, 2-g/cm^3 asteroid by one Earth radii in the available time. The power available for thrusting by the 320-kW system shown in Fig. 13 indicates that the system can thrust over the entire orbit of asteroid 2017 PDC. This is because the large solar array size provides sufficient power to operate the IBD system at 20 kW even at the asteroid's aphelion.

The required operating times for each potential IBD system are given in Fig. 14. For the 3.6-years of deflection time available, the total system operating times would be reasonable and significantly less than the 48,000 hours of ion thruster operation demonstrated on the Dawn mission [12]. The operating time for orange curve (320-kW system) would increase linearly with time because the solar array for this system provides sufficient power to thrust over asteroid 2017 PDC's entire orbit. The required operating time per thruster is given in Fig. 15. The number of thrusters is determined by taking the maximum allowed input power and dividing by the maximum power per thruster (i.e., 20 kW). In the IBD configuration a cold spare thruster is added to each side—the side facing the asteroid and the side facing away. The cold spares are not assumed to be used at any point in the mission. As the asteroid's trajectory takes the vehicle farther from the sun during IBD operations, gross system throttling would be performed by turning thrusters off in pairs to follow the available power. Finer throttling would be performed by throttling individual thrusters over their 2:1 throttle range capability. The total operating time is assumed to be equally distributed among all of the thrusters, not including the cold spares.

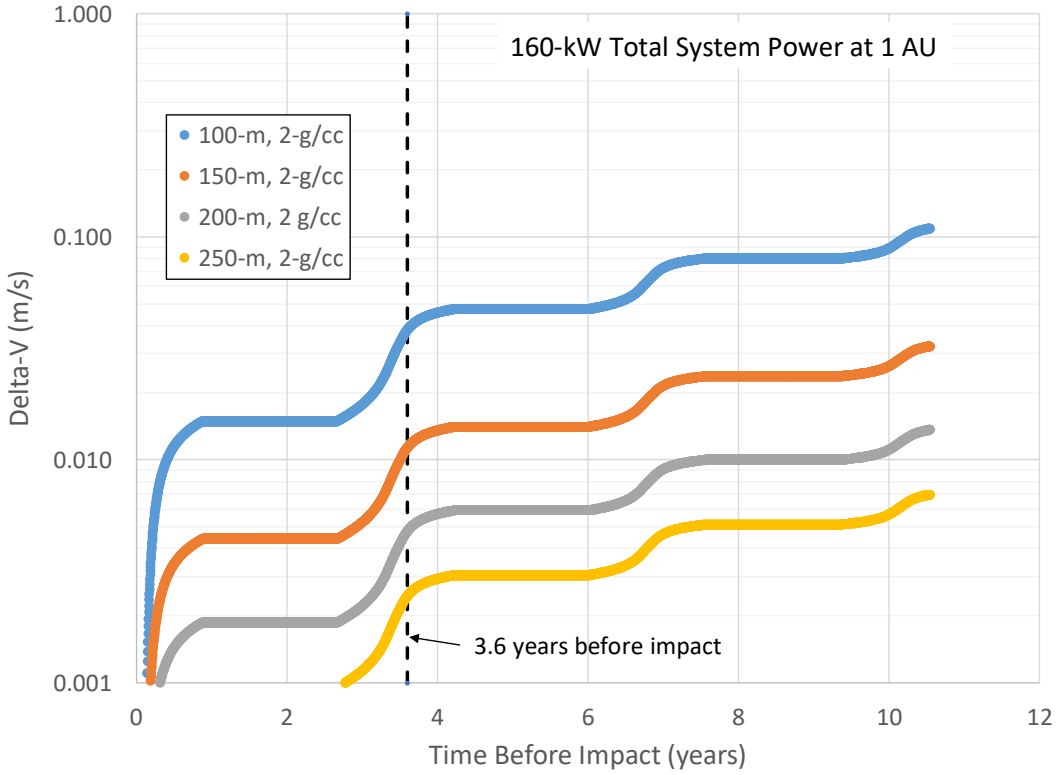

Fig. 8 Total ΔV imparted to the asteroid by the 160-kW IBD system.

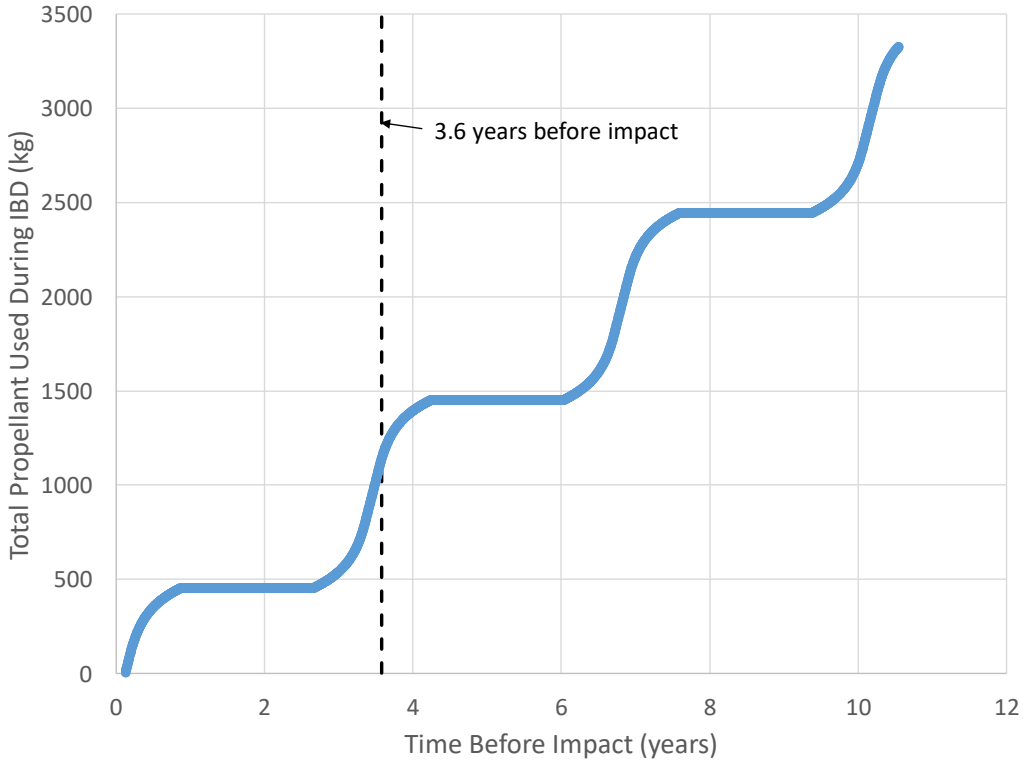

Fig. 9 Total propellant used during operations of the 160-kW IBD system.

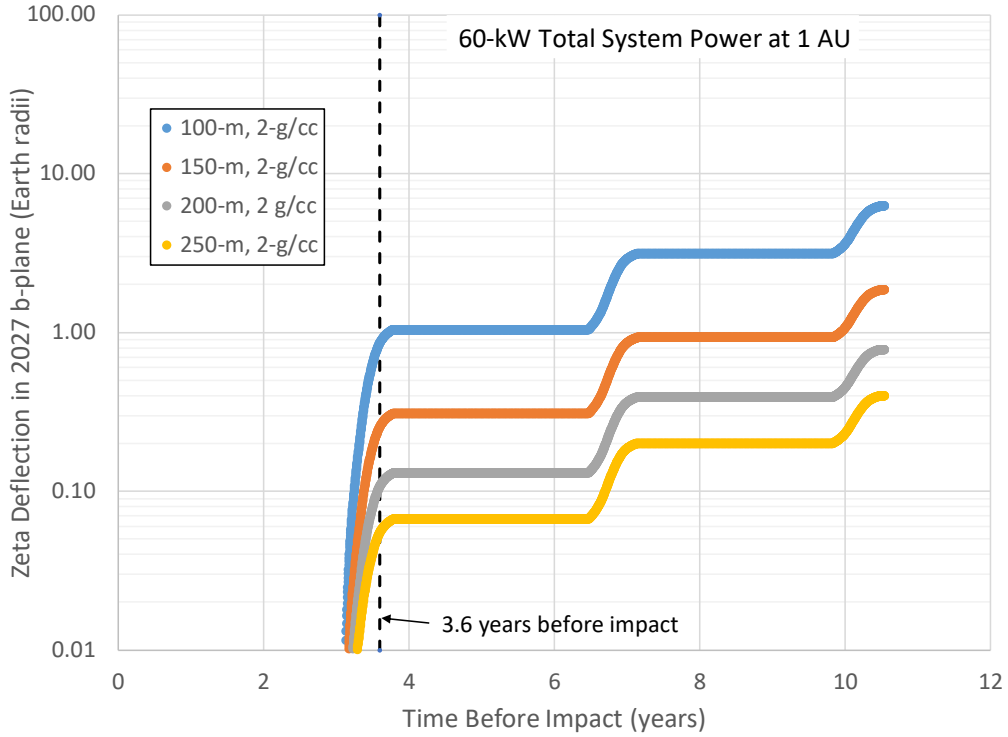

Fig. 10 Deflection capability for a 60-kW IBD system.

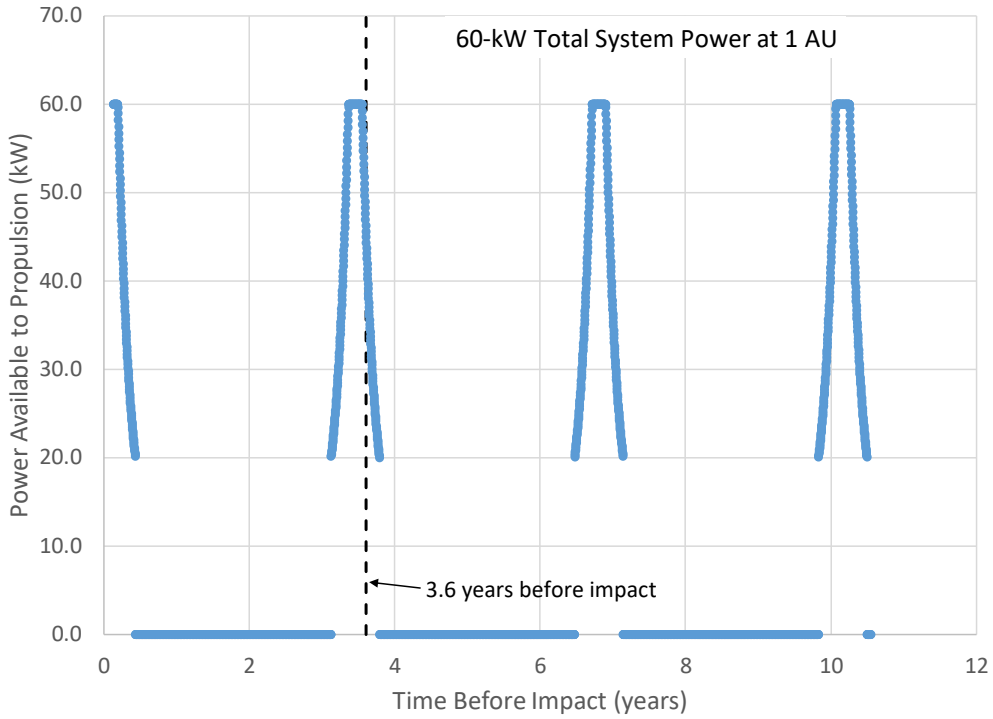

Fig. 11 Power available to the IBD propulsion system for the 60-kW spacecraft concept used in deflection results given in Fig. 10.

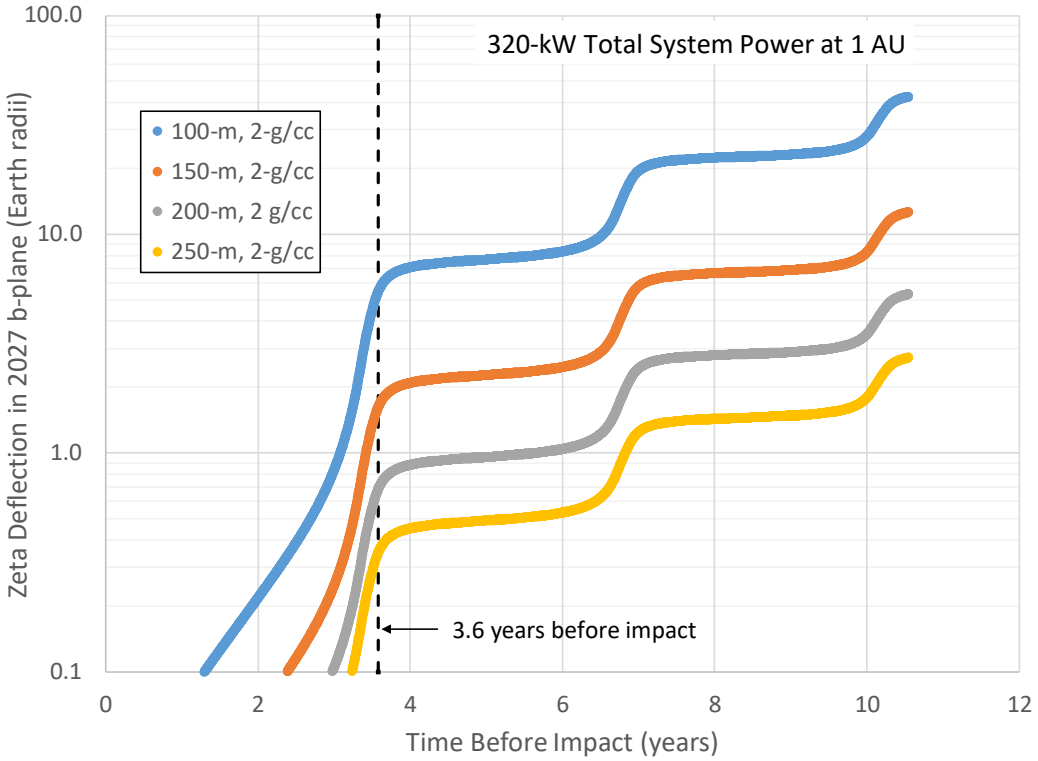

Fig. 12 Deflection capability for a 320-kW IBD system.

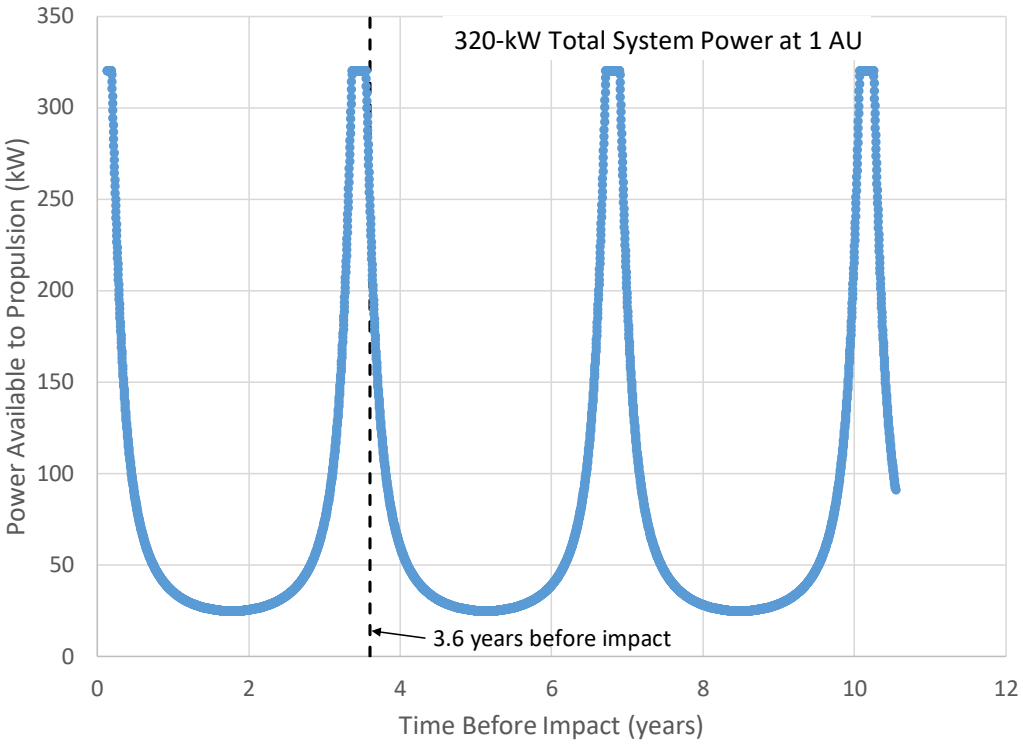

Fig. 13 Power available to the IBD propulsion system for the 60-kW spacecraft concept used in deflection results given in Fig. 12

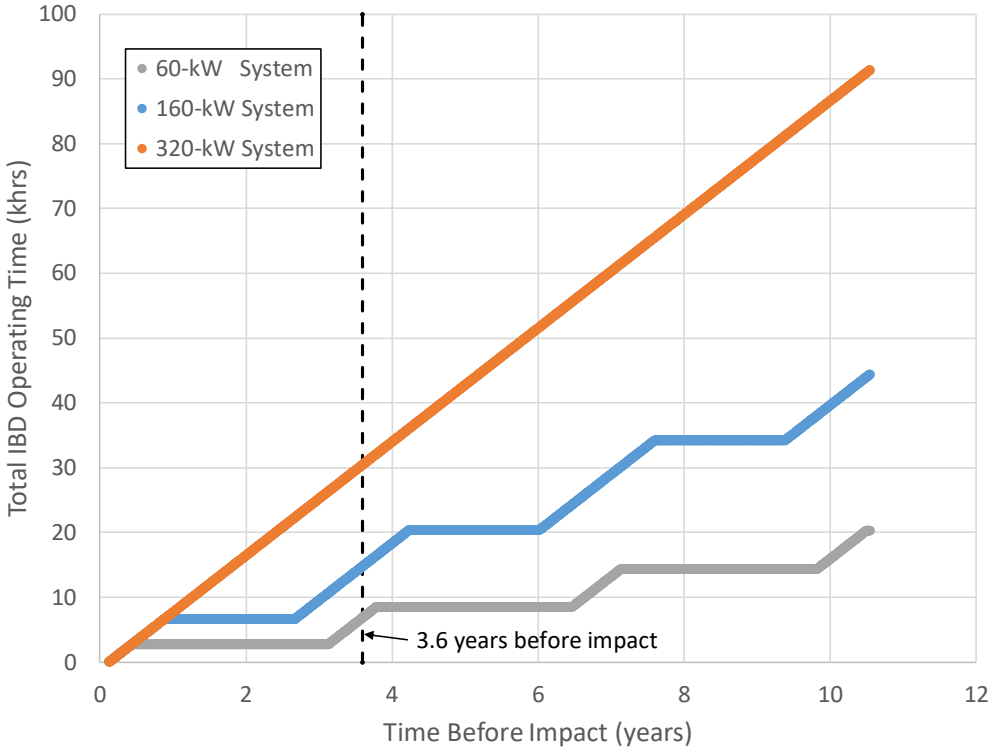

Fig. 14 The required operating time for the IBD systems is less than the 48,000 hours demonstrated by the ion propulsion system on the Dawn mission.

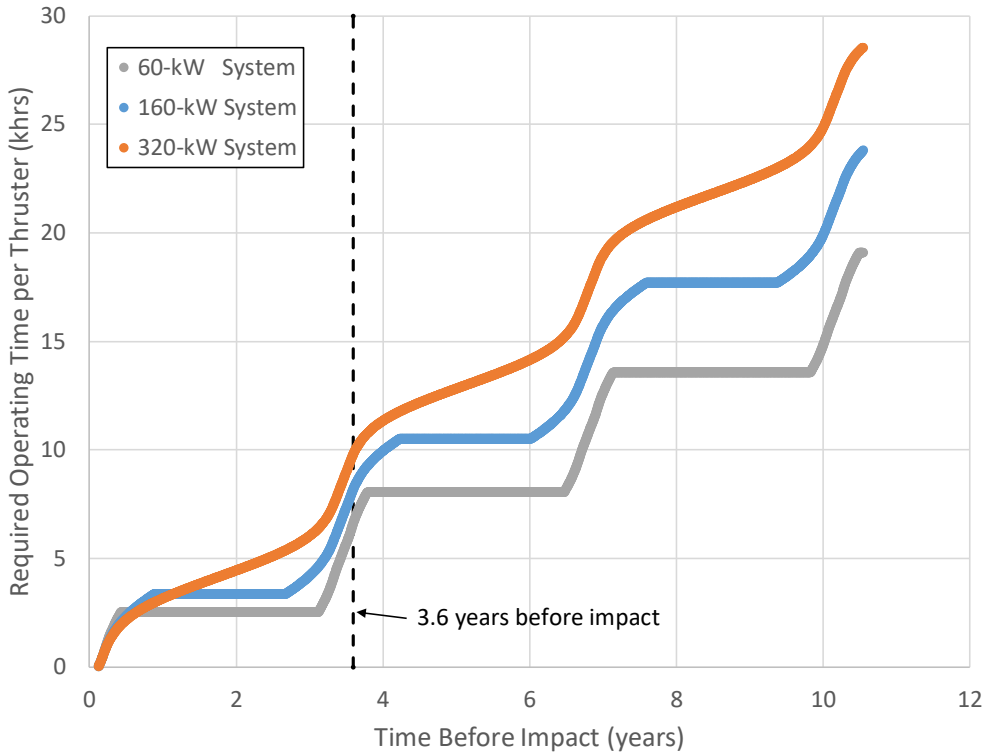

Fig. 15 The required operating time per thruster is well within the capability of gridded ion thruster technology. The Dawn ion thruster life qualification test demonstrated over 30,000 hours of thruster operation [13]. The NEXIS ion thruster design life was 87,000 hours [10].

The thruster operating times, as indicated in Fig. 15, would be less than 10,000 hours for the 3.6 years of available deflection time. Significantly, even if a full ten years prior to impact were available for deflection, the total operating time per thruster for the 160-kW IBD vehicle would still be less than ~20,000 hours. This is well within the capability of the NEXIS ion thruster, which was being developed to meet a lifetime requirement of 87,000 hrs [10]. The robust life characteristics of the NEXIS thruster suggest that it's flight development could proceed immediately with a high probability of success in meeting the life requirements of a potential near-term IBD mission such as the deflection of asteroid 2017 PDC.

Comparison with Gravity Tractor and Enhanced Gravity Tractor Concepts

In this section, the potential IBD performance is compared to two other slow-push planetary defense concepts: the conventional gravity tractor, and the enhanced gravity tractor.

Gravity Tractor (GT)

The coupling force for a conventional gravity tractor is severely limiting for asteroids in the size range of 2017 PDC, i.e., 100 m to 250 m diameter. The forces applied to asteroids of different diameters (assuming a density of 2 g/cm^3) by a gravity tractor for a 7,000-kg spacecraft and a 60-kW electric propulsion system, are given in Fig. 16. Also shown in this figure for comparison are the forces provided by high-power IBD systems. The IBD force levels can be much greater than those provided by the gravity tractor and would be independent of the asteroid size.

The deflection capability of a standard gravity tractor is given in Fig. 17. This figure indicates that a conventional gravity tractor would not come close to being able to deflect the asteroid by at least one Earth radius within the available time. More than a decade of gravity tractoring would be required to deflect even a 100-m size asteroid.

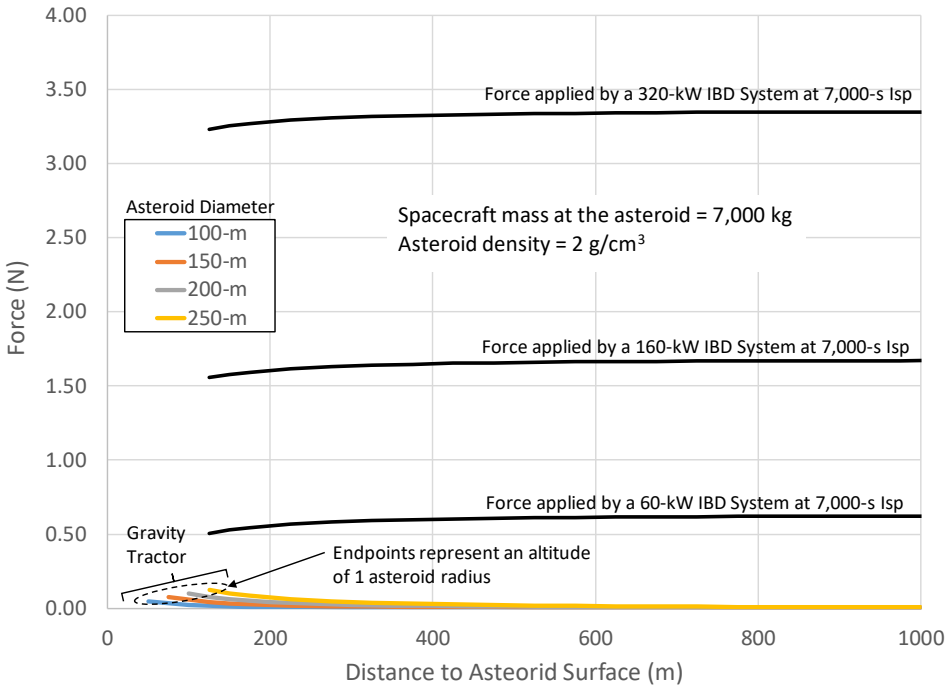

Fig. 16 High-power IBD systems have the potential to provide much higher forces to the asteroid than a conventional gravity tractor. The gravity tractor systems are assumed to have a spacecraft mass of 7,000 kg and operate at a minimum altitude of one asteroid radius. The asteroids are all assumed to have densities of 2 g/cm^3.

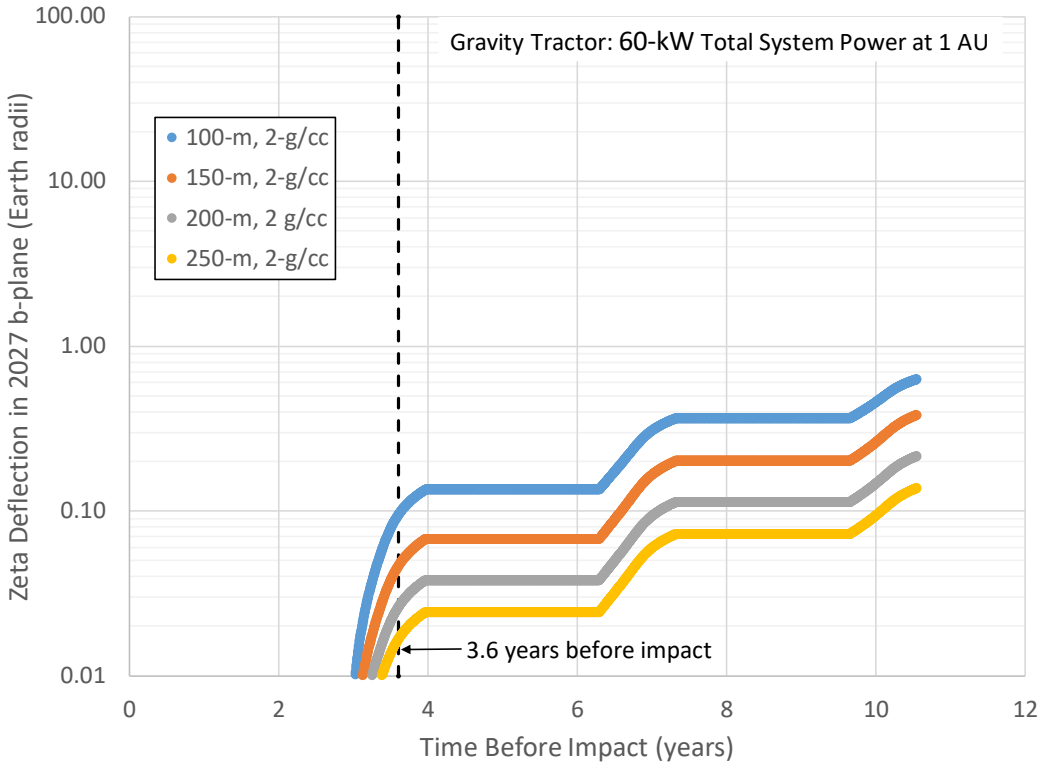

Fig. 17 Deflection capability of a 60-kW gravity tractor assuming a 10,000-kg spacecraft and a minimum spacecraft altitude of one asteroid radius.

Enhanced Gravity Tractor (EGT)

The enhanced gravity tractor method acquires mass from the asteroid to be deflected in order to increase or enhance the gravitational attraction between the spacecraft and the asteroid. This enables EGT systems to apply significantly greater forces to the asteroid than are possible with a standard gravity tractor system. In general, EGT systems seek to acquire sufficient mass to be able to use the full thrust capability of the onboard SEP system. With this approach, EGT systems can provide force levels comparable to high-power IBD systems, but the system level requirements are significantly different. This is illustrated in Fig. 18 where an EGT system was configured to provide the same performance as a 160-kW IBD system (as given in Fig. 6). To provide the deflection performance given in Fig. 18, an EGT vehicle with a 60-kW electric propulsion system operating at a specific impulse of 2800 s is required. In addition, the EGT vehicle must include the hardware necessary to acquire and store 230,000 kg of asteroid material. The EGT vehicle including the mass of the asteroid material acquisition and storage hardware must be delivered to the asteroid earlier than the IBD vehicle. The earlier arrival of the EGT vehicle is necessary to allow time for the acquisition of the necessary mass from the asteroid. If the EGT vehicle arrives at the same time as the IBD vehicle, i.e., 3.6 years before impact, and it takes six months to acquire the necessary mass, which is not an unreasonable duration, then the EGT performance will decrease by two orders of magnitude as indicated in Fig. 18. The propellant required for each system is shown in Fig. 19.

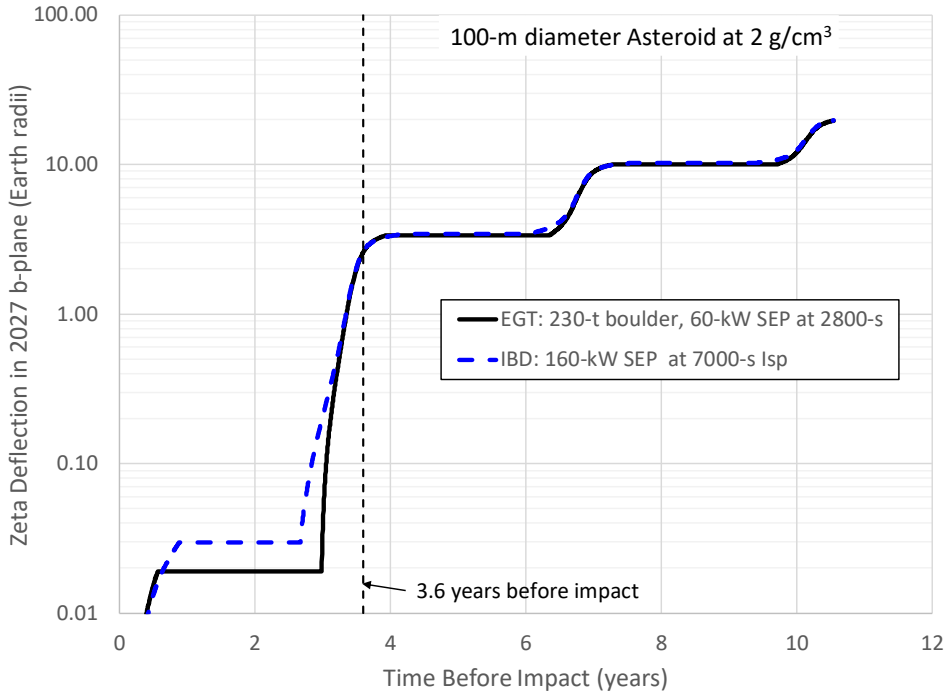

Fig. 18 Both EGT and IBD can provide the same deflection capability, but with significantly different system requirements. The EGT system is assumed to be capable of acquiring 230,000 kg of asteroid material prior to initiation of tractoring with a 60-kW, 2800-s SEP system. The IBD system is assumed to operate at a maximum input power of 160 kW with a specific impulse of 7000 s, but can initiate IBD deflection immediately after arrival. Assuming the EGT system could arrive at the asteroid 3.6 years before impact it would still require time to collect the 230,000 kg of asteroid material it needs before tractoring. If this process requires six months then the deflection provided by the EGT system will decrease by two orders of magnitude.

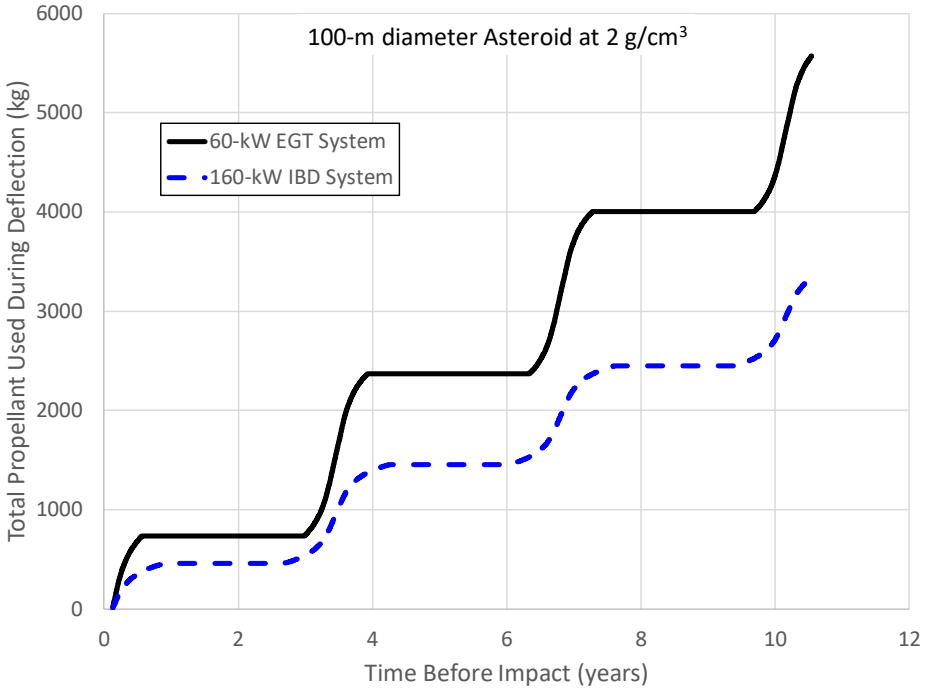

Fig. 19 Propellant required for deflection of 2017 PDC if it were 100-m diameter at 2 g/cm3. The 160-kW IBD system actually uses less propellant because of its much higher specific impulse, 7000 s, than the 60-kW EGT with a specific impulse of 2800 s.

Multiple, Simultaneous IBD Vehicles

Multiple, simultaneously operating IBD vehicles are likely to be required for the deflection of an actual threat object for several reasons. First, a realistic deflection strategy would likely not rely on the successful operation of a single deflection vehicle even if it were single-fault-tolerate. Second, additional vehicles may be used to improve the robustness of the deflection system to unknowns. For example, even if a precursor flyby mission successfully constrains the size of the asteroid, its density will still have significant uncertainty. A factor of two uncertainty in the density could be accommodated by increasing the number of IBD spacecraft. Therefore, it is of interest to investigate how multiple IBD vehicles could operate simultaneously at the same asteroid.

Once multiple vehicles are delivered to the proximity of the asteroid, the spacecraft must have both situational awareness and control of where they are with respect to the asteroid and with respect to the other IBD vehicles. Safety and sustainability of the formation are principal to the success of this approach. The next subsections review how a formation-flying constellation would be selected and the relative guidance, navigation, and control approach.

Formation Flying Constellation Selection

Flying vehicles in formation relative to the asteroid is a challenging problem requiring placement of the individual spacecraft to optimize total imparted delta-V to the asteroid, while minimizing the potential for plume interaction between vehicles and collision risk between each spacecraft with the asteroid and with respect to one another. Therefore, an IBD constellation can be constructed by solving the following optimization problem:

$$\begin{aligned} & \max \Delta \mathrm{v} \\ \text{s.t.} \quad & l_{\mathrm{a,min}} < l_{\mathrm{a}}^{\mathrm{i}}, \forall \mathrm{i} \\ & l_{s,min} < l_s^{ij}, \forall i,j \end{aligned}$$

where l_a^i is the range between the asteroid a i^{th} spacecraft and l_s^{ij} is the range between the i^{th} and j^{th} spacecraft. A discussion of what is driving the limits is pertinent.

The minimum asteroid-spacecraft range, $l_{\mathrm{a,min}}$, is driven by the need to minimize impact risk while flying in proximity of the asteroid. It can be derived by specifying a minimum free-fall (unthrusted) time-to-collision and determining the resulting range. There is no direct constraint on the maximum asteroid-spacecraft distance, but closer distances are preferred due to momentum exchange efficiency and plume divergence considerations.

The minimum spacecraft-to-spacecraft range, $l_{s,min}$, is driven by the need to minimize impact risk between spacecraft in the constellation. The dimensions of the spacecraft along the solar-array axis may be quite large and even approach the diameter of the asteroid in the smallest case. This also drives the need for formation-flying techniques where intra-spacecraft state knowledge and control is necessary.

For small IBD constellation sizes, the constraints can be inspected graphically, as shown in Fig. 20 and 21. Figure 20 depicts the spacecraft-to-asteroid range vs asteroid mass with color defining the duration to passively descend (without thrusting) down to a 250 m range from the initial condition defined by the separation distance. This provides a mechanism for choosing the minimum spacecraft-asteroid range based on free-fall duration, which is a surrogate metric for how long the constellation can be unattended without ground interaction. For the largest asteroid (250 m radius with 4 g/cm^3 density), this free-fall duration is only 1 to 6 hours across the range of study, which may be shorter than the worst-case ground communication outage, driving a fully autonomous fault detection and abort to safe range (see GN&C discussion for implications).

For the case of a 2-deg thruster plume divergence cone, the spacecraft-to-asteroid separation can be further constrained by the desire to keep the IBD plume on the asteroid. For the minimum asteroid diameter (100 m), this equates to an upper bound of approximately 1500 m. Therefore, given the desire to maximize the range, 1500 m spacecraft-to-asteroid rage will be assumed for the remainder of this analysis.

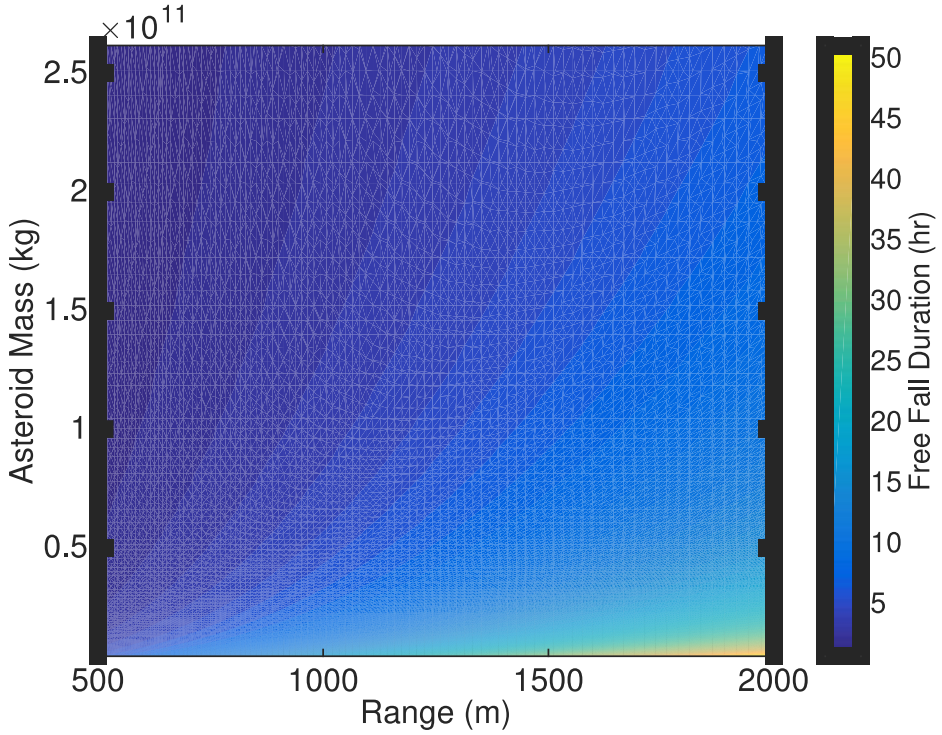

Fig. 20 Free-Fall Duration

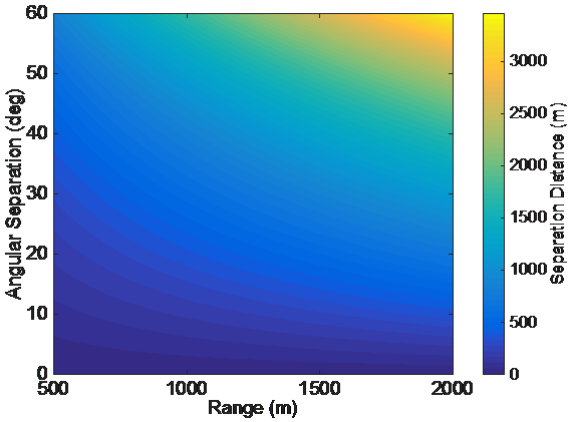

(a) Angular separation impact

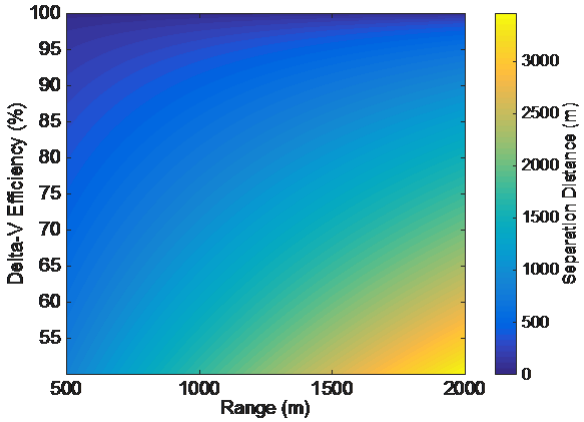

(b) Delta-V efficiency impact

Fig. 21 Spacecraft-to-Spacecraft Separation Distance

Figure 21 (a) provides a mechanism to design an inter-vehicular angular separation that results in a delta-v efficiency loss based on minimum spacecraft-to-spacecraft distance. For example, suppose the minimum spacecraft-to-spacecraft separation distance is 1000 m. At a 1500 m asteroid offset, this yields approximately 35 deg of angular separation between the vehicles. From Fig. 21 (b), this separation equates to a delta-V efficiency in the desired thrust

direction of 83%. However, for a two-vehicle constellation concept, the angular separation would be effectively half of this angle from the desired thrust direction (17.5 deg), which equates to a delta-V efficiency in the thrust direction of 95%. For a three-vehicle constellation concept, the effective delta-V efficiency would be 88%, as one vehicle would be along the desired thrust direction and the other two would be separated from that vehicle by 35 deg.

In summary, this analysis suggests the limiting case be the vehicles are situated at a range of 1500 meters from the asteroid and separated by 35 deg with respect to each other (with a vehicle centered on the desired thrust direction for odd number vehicle configurations), yielding an 88% delta-V efficiency for the baseline three-vehicle scenario. Depending on the true observed asteroid mass and size, the constellation would be refined, but the 88% delta-V efficiency provides a bound for use in deflection analysis for assurance the design can handle the worst-case scenario.

Proximity Operations Guidance, Navigation, and Control

Now that a constellation concept is designed, it is the role of the guidance, navigation, and control subsystem to deliver the vehicles to their respective asteroid-relative position and ensure the formation of vehicles relative to the asteroid surface is maintained.

If the ground could be assumed to be in constant communication with each vehicle with proper telemetry visibility, then all space situational awareness (i.e., relative navigation state) could be provided by a human element on the ground. However, this is an unrealistic scenario for a formation-flying application that will last years – driving autonomy into all elements of the GN&C subsystem.

As a fully autonomous GN&C subsystem would be required, the presence of a continuous relative navigation state is vital to any approach. The relative navigation state, in this context, is defined such that each vehicle would have knowledge of their attitude and position relative to the asteroid and also relative to every other spacecraft. There are two potential approaches to this problem, one relying on a direct measurement and the other an indirect derived measurement. In the indirect approach, each vehicle would have the means to only measure their state relative to the asteroid. Inter-spacecraft communication would be relied upon to broadcast each vehicle's asteroid-relative, which would be used to derive a measurement of spacecraft-to-spacecraft position and attitude. Alternatively, by directly measuring the relative state of all spacecraft and the asteroid, more robustness would be added but at the burden of computational and algorithmic complexity and sensor capability.

There are several techniques in application and in the literature for providing a relative-state measurement in asteroid applications. All of these techniques rely on correlation of onboard imagery to available maps of the asteroid surface. For example, the natural feature tracking algorithm of Osiris-Rex correlates features on the asteroid surface to those found in onboard imagery to generate a relative position estimate [14]. Retina operates on a similar principle and was to be applied for the boulder capture for the ARRM mission [15]. A similar map-relative location approach is also under development for the Lander Vision System of the Mars 2020 mission [16,17].

Pedigree also exists for the spacecraft-to-spacecraft relative state measurement. For example, a Lidar-based approach was flown on the XSS-11 mission [18]. The Raven mission to the International Space Station developed both a Lidar-based approach (FPose) and an image-relative navigation approach (GNIFR), where these algorithms are intended to be used for future satellite servicing missions [19]. For the application of IBD deflection of an asteroid with multiple vehicles flying in formation, a Lidar-based measurement is considered more robust, because it is an active sensor and less dependent on the lighting conditions, which may be dictated by other mission aspects and unfavorable for the measurement of other spacecraft states.

The translational guidance approach for the IBD formation would be quite simple – generate a reference position for the controller to maintain a hover over a specific latitude, longitude, and altitude. The attitude guidance would then generate the commands to maintain the thrust vector along the desired delta-V direction in heliocentric RTN (radial-transverse-normal) coordinates. Clearly, the translational and attitude guidance would be coupled and must be treated accordingly.

Pre-cursor Missions

It is clear from the above analysis that the ability of an IBD vehicle to successfully deflect the asteroid is highly dependent on the asteroid's size and density. Of these two, size uncertainty is much more important as it effects mass uncertainty as a cube of the radius while density is linear. A pre-cursor flyby spacecraft with a camera could determine the asteroid dimensions and a spectrometer could be used to roughly constrain density. However, an orbiter would be required to fully determine the mass and density of an asteroid.

In order to be able to launch a pre-cursor survey spacecraft early, it is assumed that a commercial satellite with SEP could be procured, retrofitted with a instruments, and launched on a Falcon 9 (or more capable) rocket by mid 2018. Figure 22 shows example flyby and rendezvous trajectories assuming a spacecraft similar to the Boeing 702SP and a Falcon-9-class launcher. Both cases would depart in July 2018, but the flyby spacecraft would arrive in July 2019 while the rendezvous mission would take until November 2020.

Early shape information from images acquired on a flyby would probably be more valuable than the more complete information that could be obtained by a later orbiter. However, given that the PDC 2017 asteroid would be extremely hazardous, there should be sufficient resources to launch both flyby and rendezvous precursors vehicles. The flyby mission would provide rough asteroid shape data in 2019 that could be used in the design of the IBD spacecraft. The rendezvous mission would later provide more detailed shape, density, and gravity data that could be used for planning the operations of an IBD spacecraft.

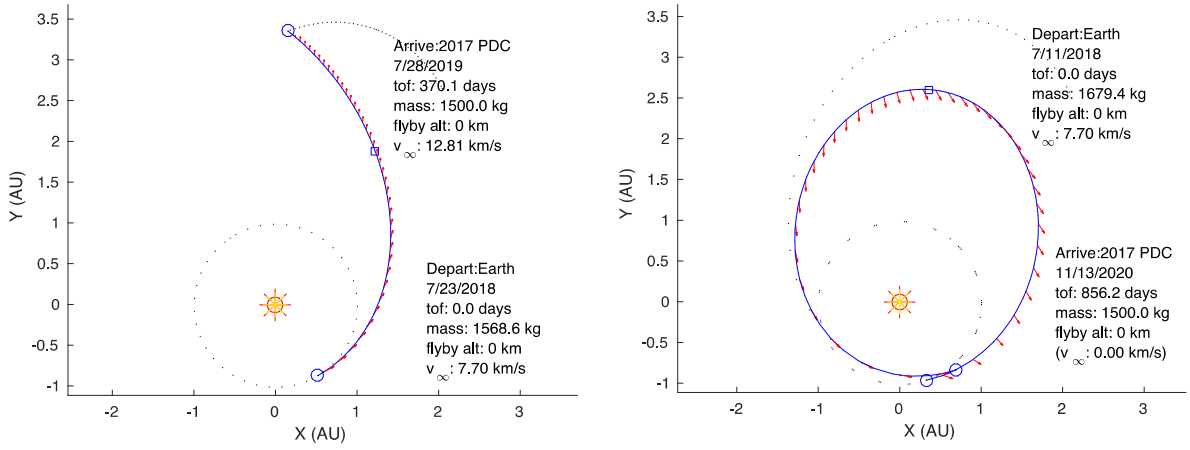

Fig. 22 Example pre-cursor flyby (left) and rendezvous (right) missions, assuming a 702SP-like spacecraft and a Falcon-9-like launch vehicle.

Example Mission Concept Timeline

Figure 23 shows two opportunities for an earlier launch than the 2021 launch given in Fig. 5. The trajectories in Fig. 23 assume a 160-kW IBD spacecraft and a Falcon Heavy or more capable launch vehicle. The shortest flight time is a July 2019 launch that would only take 1.2 years to reach the asteroid. However this launch is too soon for the development of a new vehicle and would only be practical if the IBD spacecraft were already developed or perhaps if

it could be built from an already-existing design. The 2020 and 2021 launch opportunities have flight times of 2.4 and 2.6 years respectively. The 2020 case would provide enough time for 4.8 years of deflection, but only about 3 years to develop and build the IBD spacecraft. The 2021 case provides an extra year before launch, but only allows 3.6 years for deflection.

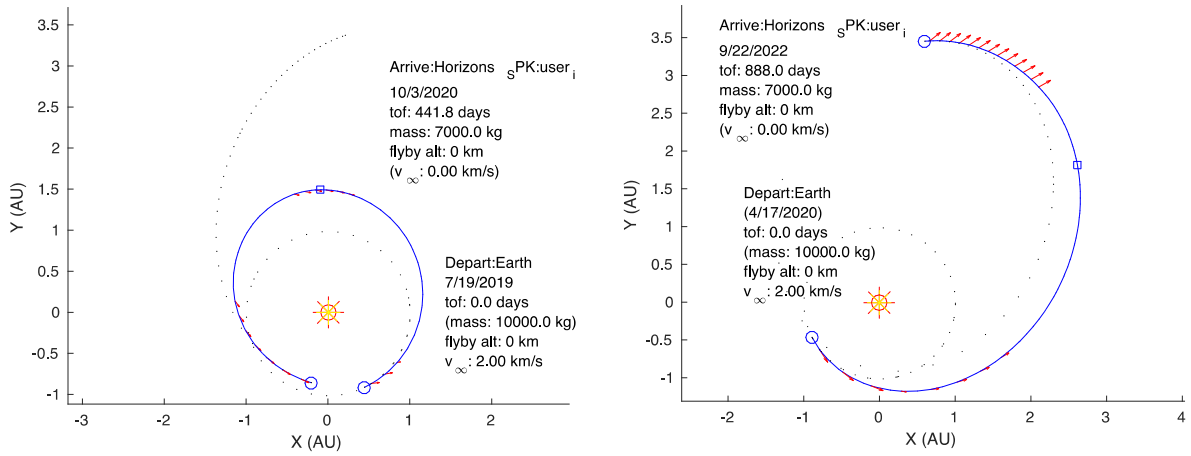

Fig. 23 Example 160 kW IBD spacecraft trajectories for 2019 (left), 2020 (middle) launches, assuming a Falcon-Heavy-like launch vehicle. The trajectory for a 2021 launch is given in Fig. 5.

Technology Development Needs

The NASA appropriations bill of 2005 mandated that NASA perform a survey to discover and track all NEOs greater than 140 meters in diameter. After this survey is complete and if nothing is found on a collision course with Earth, then the impact risk will be dominated by Tunguska-scale objects, i.e., objects that are tens of meters in diameter [20]. IBD is particularly well suited to the deflection of objects in the size range of 50 m to 100 m diameter. For example, as indicated in Fig. 6, if asteroid 2017 PDC were 100 m diameter with a density of 2 g/cm^3, it would only take approximately two months of IBD operations for the 160-kW IBD vehicle to deflect it by one Earth radius, assuming that deflection operations began 3.6 years before impact. Deflection of objects smaller than 100 m would be easier and could be performed with the same IBD vehicle. The only change required would be an operational one. For smaller objects, the spacecraft-to-asteroid surface would have to be reduced according to Fig. 2 in order to maximize the fraction of the ion beam that impacts the asteroid.

Since smaller objects, those in the size range of 50 m to 100 m diameter, are expected to be characterized by less warning time before impact, the following two relatively affordable steps could be taken to reduce the time necessary to build and launch an IBD vehicle. First, the development of the NEXIS ion propulsion technology could be completed and flight qualified. This would include fabrication and test of an engineering model thruster with flat carbon-carbon grids and an engineering model of the power processing unit (PPU) required to drive the thruster. Tests would include characterization of the ion beam divergence angle over the throttle range, followed by a long-duration test of at least 15,000 hours. A qualification model thruster and PPU would then be fabricated and flight qualified. Doing these things would make this technology immediately available for implementation on an IBD vehicle. Second, a project-level activity could be performed that would execute the Phase A and Phase B activities of a typical flight project implementation. The end result of this effort would be a spacecraft design concept mature enough to proceed immediately into Phase C/D should the need arise. The above two activities, hardware maturation at the component level and concept maturation at the flight system level, would greatly improve the ability to respond to a near-term threat for a modest cost.

Conclusions

The performance of an ion beam deflection (IBD) system has less dependency on the characteristics of the threat object than any other potential asteroid deflection technique. This feature alone makes IBD an attractive technique. Nevertheless, like all deflection technologies it is very sensitive to the mass of the object to be deflected and the time available for that deflection. To determine the time available for deflection of the hypothetical asteroid 2017 PDC the analyses presented herein include an allocation of four years for the design, fabrication, test and launch of the IBD vehicle, and 2.6 years for the heliocentric transfer to rendezvous with the asteroid. This leaves approximately 3.6 years to perform the deflection. A 160-kW IBD system, operating with a specific impulse of 7,000 s, could deflect asteroid 2017 PDC by at least one Earth radius provided the asteroid was less than approximately 140 m diameter and had a density of 2 g/cm^3 or less. If the asteroid diameter were larger and/or had a greater density, then either more time would be required for the deflection or a higher power system would be required, or both.

IBD based on high-power solar electric propulsion is particularly well suited for the deflections of near-Earth asteroids in the size range of 50 m to 100 m diameter. Since this size range may represent the greatest impact hazard it would be prudent to pursue the development of an IBD capability based on the high-power SEP systems that NASA already is considering for future human exploration of Mars. Significantly, a 160-kW IBD system is of a power level that is believed to be comparable to that being considered for NASA's Deep Space Transport vehicle. To greatly improve the response time to a newly discovered threat object in the 50- to 100-m size range, the development of the NEXIS ion thruster needed for a high-power IBD system could be completed and flight qualified. In addition, a project-level activity could be conducted to mature a high-power IBD vehicle concept by executing the first two phases (Phase A and B) of a typical flight implementation. These activities0 would reduce that response time by at least a year while lowering the implementation risk.

Acknowledgements

The research described in this paper was carried out in part at the Jet Propulsion Laboratory, California Institute of Technology, under a contract with the National Aeronautics and Space Administration, and at the NASA Langley Research Center.

References

1. Rayman, M.D., et al., "Results from the Deep Space 1 Technology Validation Mission," 50th International Astronautical Congress, Amsterdam, The Netherlands, 4-8 October, 1999, IAA-99-IAA.11.2.01, Acta Astronautica 47, p. 475 (2000).
2. G. Saccoccia, D. Estublier, G. Racca " SMART-1: A Technology Demonstration Mission for Science Using Electric Propulsion", AIAA-98-3330, 34th AIAA/SAE/ASME/ASEE Joint Propulsion Conference and Exhibit, July 13th-5th, 1998 / Cleveland, OH.
3. Thomas, V.C., et al., "The Dawn Spacecraft," Space Sci Rev (2011) 163:175–249, DOI 10.1007/s11214-011-9852-2.
4. Kuninaka, H., et al., "Powered Flight of Hayabusa in Deep Space," AIAA 2006-4318, 42nd AIAA/ASME/SAE/ASEE Joint Propulsion Conference & Exhibit 9 - 12 July 2006, Sacramento, California.
5. Tsuda, Y., et al., "System design of the Hayabusa 2—Asteroid sample return mission to 1999 JU3," *Acta Astronautica*, Volume 19, Oct-Nov 2013, pg 356-362.
6. https://www.nasa.gov/sites/default/files/atoms/files/heo_update_tagged.pdf
7. Bombardelli, C., et al., "The ion beam shepherd: A new concept for asteroid deflection," presented at the 2011 IAA Planetary Defense Conference, 09-12 May 2011.

8. Kitamura, S., “Large Space Debris Reorbiter Using Ion Beam Irradiation,” IAC-10-A6.4.8, 61st International Astronautical Congress, September 2010.
9. Brophy, J.R., “Advanced Solar Electric Propulsion for Planetary Defense,” IEPC-2015-64, Presented at Joint Conference of 30th International Symposium on Space Technology and Science, 34th International Electric Propulsion Conference and 6th Nano-satellite Symposium, Hyogo-Kobe, Japan, July 4 – 10, 2015
10. Polk, J.E., et al., “Performance and Wear Test Results for a 20-kW-Class Ion Engine with Carbon-Carbon Grids, AIAA 2005-4393, presented at the 41st AIAA/ASME/SAE/ASEE Joint Propulsion Conference & Exhibit, 10-13 July 2005, Tucson, AZ.
11. Chodas, Paul W., Jet Propulsion Laboratory, personal communication.
12. Garner, C.E., and Rayman, M.D., “In-flight Operation of the Dawn Ion Propulsion System Through Completion of Dawn’s Primary Mission,” AIAA 2016-4539, AIAA Propulsion and Energy Forum, 52nd AIAA/SAE/ASEE Joint Propulsion Conference, July 25-27, 2016, Salt Lake City, UT.
13. Sengupta, A., et al., “An Overview of the Results from the 30,000 hr Life Test of Deep Space 1 Flight Spare Ion Thruster,” AIAA 2004-3608, 40th AIAA/ASME/SAE/ASEE Joint Propulsion Conference, 11-14 July 2004, Fort Lauderdale, FL.
14. Lorenz, D.A., et al., “Lessons Learned from OSIRIS-Rex Autonomous Navigation Using Natural Feature Tracking,” IEEE Aerospace Conference, March 2017, Big Sky, MT.
15. Wright, C. A., Van Eepoel, J., Liounis, A., Shoemaker, M., DeWeese, K., and Getzandanner, K., “Relative Terrain Imaging Navigation (RETINA) Tool for the Asteroid Redirect Robotic Mission (ARRM),” 39th AAS Guidance, Navigation, and Control Conference, Breckenridge, CO, Feb. 2016.
16. Johnson, A., Bergh, C., Cheng, Y., Clouse, D., Gostelow, K., Ishikawa, K., and Park, S., “Design and ground test results for the lander vision system,” 36th AAS Guidance and Control Conference, Breckenridge, CO, Feb. 2013.
17. https://www.nasa.gov/centers/armstrong/features/fresh_eyes_on_mars.html
18. Allen, Andrew CM, et al. "Rendezvous lidar sensor system for terminal rendezvous, capture, and berthing to the International Space Station," SPIE Defense and Security Symposium. International Society for Optics and Photonics, 2008.
19. Strube, M., et al. "Raven: An On-Orbit Relative Navigation Demonstration Using International Space Station Visiting Vehicles," 2015.
20. Boslough, M., Brown, P., and Harris, A., “Updated Population and Risk Assessment for Airburst from Near-Earth Objects (NEOs),” IEEE Aerospace Conference, March 2015, Big Sky, MT.